ACS Sustainable Chemistry & Engineering

pubs.acs.org/journal/ascecg

Research Article

Cobalt-Based Quasi-Metal–Organic Framework as a Tandem Catalyst for Room-Temperature Open-Air One-Pot Synthesis of Imines

Minoo Bagheri, Mohammad Yaser Masoomi,* Esther Domínguez, and Hermenegildo García*

Cite This: *ACS Sustainable Chem. Eng.* 2021, 9, 10611–10619

Read Online

ACCESS | Metrics & More | Article Recommendations | Supporting Information

ABSTRACT: The catalytic activity of MOFs derives in a large extent from defects. To generate these defects, a cobalt-based metal–organic framework TMU-10, $[Co_6(oba)_5(OH)_2(H_2O)_2(DMF)_4]_n \cdot 2DMF$ has been subjected in the present study to controlled thermal treatment under air at different temperatures ranging from 100 to 700 °C. This treatment produces the removal of ligands, generation of structural defects, and additional porosity in an extent that depends on the conditions of the thermal treatment. The resulting defective materials, denoted according to the literature as *quasi*-MOFs, were subsequently employed as heterogeneous tandem catalysts in the one-pot synthesis of *N*-benzylideneaniline from aniline and benzyl alcohol in open air as a terminal oxidant at 60 °C under solvent-, base-, and dehydrating agent-free conditions. The *quasi*-TMU-10 framework obtained at 300 °C (QT-300) can efficiently promote imine synthesis within 2 h, forming water as the only byproduct. Unsaturated cobalt sites and the presence of micro- and mesopores in QT-300 are responsible for this excellent catalytic performance as tandem catalysts. The influence on QT-300 catalytic activity of catalyst amount, reactant ratio, and reaction temperature was investigated, as well as the stability and recyclability of the catalyst. The one-pot imine formation promoted by QT-300 follows alcohol aerobic oxidation and subsequent anaerobic condensation of the aldehyde intermediate with aniline.

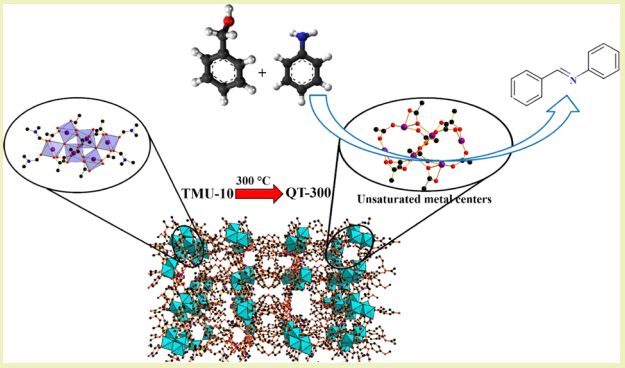

KEYWORDS: *tandem catalysis, quasi-metal–organic frameworks, partial deligandation, pore engineering, imine formation*

INTRODUCTION

Tandem catalysts, as multifunctional materials able to catalyze multiple reactions in one step, have received much attention in the last two decades for multiple-step syntheses due to their advantages in terms of simpler workup and process intensification.[1] By having an active C=N bond, imines are key intermediates in the synthesis of pharmaceuticals, fine chemicals, and biologically active heterocyclic compounds, such as α-amino acids and α-amino alcohols.[2] Imine reactivity includes reduction, addition, condensation, and multicomponent reactions.[3,4]

Several synthetic routes are described in the literature for imine synthesis.[5] However, in the past decade, more attention has been paid to the direct synthesis of imines through one-pot processes from alcohols and amines via an oxidative reaction, which diminishes energy consumption and wastes as well as minimizes purification steps.[6] Three green techniques including the cross-coupling of alcohols with amines, the self-coupling of primary amines, and the oxidative dehydrogenation of secondary amines have been widely employed for imine synthesis due to the availability of the starting materials and also employment of air or O_2 as the terminal oxidant, instead of environmentally harmful chemical oxidants.[7,8] Among them, the oxidative cross-coupling of alcohols with amines is one of the most convenient processes for imine preparation. The salient features of the mentioned method are formation of water as the only byproduct of the process and synthesis of different symmetric and asymmetric imines by combining various starting materials.[2,6]

Metal–organic frameworks (MOFs) are a class of porous crystalline materials containing metal ions or metal clusters coordinated to rigid bi- or multipodal organic ligands generating a considerable internal void space.[9] In some cases, the pores in a framework are filled with guest molecules (often solvents), whose removal can generate coordinatively unsaturated positions around the metal nodes. These features of MOFs are of interest for application in gas storage, gas separation, gas purification, catalysis, and supercapacitors.[1,10,11]

Received: April 27, 2021
Revised: July 19, 2021
Published: July 28, 2021

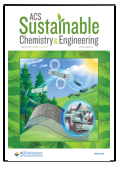

Catalytic active sites in MOFs can be located at the metal nodes, linkers, and/or within the pores, there being appropriate strategies to activate or implement these active sites.[9,12] Active sites are accessible to substrates and reagents through the pores. Pore engineering is an important way to obtain catalytically active MOFs while modulating site accessibility.[13−15] Recently, much attention has been paid to the role of defects on the catalytic activity of MOFs. Since structural defects may result in the presence of coordinatively unsaturated positions around metal ions, able to coordinate with substrates and reagents, efforts have been made for developing strategies to create defects. One of these methodologies is the generation of structural defects by partial deligandation under controlled thermal treatment to create Lewis acid centers.[16,17] The term "*quasi*-MOFs" (Q-MOFs) has been used to indicate the resulting damaged structures that can be considered to represent an intermediate stage between metal oxides and perfect MOFs with features and advantages of both.[16−19]

Herein, we have applied a Q-MOF based on the cobalt-MOF (TMU-10) as a solid tandem catalyst for the one-pot direct coupling of alcohol and amine to the corresponding imine in the absence of any base or chemical oxidant. Our strategy relies on the generation of Lewis acid sites and pore engineering by creation of defects on the TMU-10 framework. Optimal thermal deligandation causes an extra high density of open cobalt sites with simultaneous formation of both micro- and mesopores after partial damage of the TMU-10 network. Our approach renders an efficient solid catalyst for the direct, green, and easy one-pot synthesis of imine with air as the terminal oxidant under solvent-free conditions and at room temperature. The selection of TMU-10 as a precursor offers the advantage of a reliable and convenient synthesis from affordable ligands, combined with the general catalytic activity of Co MOFs in oxidation reactions.

It was anticipated that open cobalt sites as Lewis acid centers can activate oxygen molecules of air, promoting alcohol oxidation and the subsequent condensation steps. It has also been proven that a proper metal catalyst can facilitate the oxidation of both alcohol and amine.[6] In contrast to most metal oxides, catalysts based on quasi-MOFs do not undergo particle aggregation, exhibiting a uniform distribution of active metal catalytic sites throughout the Q-MOF framework. In this strategy, porosity and the crystal structure of the parent TMU-10 are partially intact, making possible reactant diffusion to the active sites.

Some cobalt-based catalysts have been applied for imine synthesis,[20−24] and some MOFs with or without cocatalysts have been also studied as catalysts for this reaction.[25−28] However, to the best of our knowledge, there is no previous report showing that thermal deligandation is a convenient way to prepare even more efficient catalysts for the synthesis of imines under mild and green conditions.

TMU-10, $[Co_6(oba)_5(OH)_2(H_2O)_2(DMF)_4]_n{\cdot}2DMF$ (H_2oba = 4,4′-oxybisbenzoic acid), is a Co-based MOF with high thermal stability in which there are hexanuclear secondary building units (SBUs) of cobalt centers.[29] Herein, it will be described how partial deligandation on TMU-10 can produce a highly active noble metal-free tandem catalyst based on the Q-MOF (abbreviated as "QT-*x*" in this study), consisting of coordinatively unsaturated Lewis acid Co sites, as well as coexistence of micro- and mesopores, favoring internal diffusion for direct synthesis of imines in a one-pot process. The QTMU-10 has been prepared via partial deligandation in air at different temperatures ranging from 100 to 700 °C with a heating rate of 5 °C min^{-1}. The process removes some organic linkers, generating structural defects and coordinatively unsaturated positions around Co^{2+} ions able to act as catalytic sites. The catalytic performance of QTMU-10 significantly improves upon optimal deligandation compared to the TMU-10 precursor, the highest catalytic performance being achieved for the sample subjected to 300 °C. Available characterization data indicate that the increase of catalytic activity probably derives from simultaneous presence of micro- and mesopores, as well as the uniform and extended distribution of active Co catalytic sites across the framework and the prevention of generation of agglomerate CoOx particles. Reusability of the Q-MOF and the corresponding kinetic and thermodynamic properties have also been investigated. The results show that the combination of the hierarchical porous structure and Lewis active sites present in QTMU-10 renders a catalyst that is more active than the mere blending of the related MOF and cobalt oxide. Given the scarce number of examples on thermal deligandation to enhance the catalytic activity of MOFs, our report provides data, confirming this process as a general methodology to obtain advanced catalytic materials.

EXPERIMENTAL SECTION

Materials and Physical Techniques. All reagents and materials for the synthesis and analysis were commercially available from Aldrich and Merck Company and used without further purification. The IR spectra were recorded using Thermo Nicolet IR 100 FT-IR spectrophotometer. A PL-STA 1500 apparatus was used for measurement of thermal behavior, heating the samples at the rate of 10 °C min^{-1} in a static nitrogen atmosphere. Powder X-ray diffraction (PXRD) patterns were acquired with a Philips X'pert diffractometer with monochromated Cu Kα radiation. Elemental analyses were carried out using a CHNS Thermo Scientific Flash 2000 elemental analyzer. Sorption studies of N_2 at 77 K were performed using the TriStar II 3020 surface area analyzer from Micrometrics Instrument Corporation and BELSORP-mini II from LMS Instruments Co., Ltd. All samples were activated at 120 °C for 14 h under vacuum before N_2 adsorption. The pore-size distributions were calculated from the adsorption branch of the N_2 isotherms according to the Barrett−Joyner−Halenda (BJH) method. X-ray photoelectron spectroscopy (XPS) measurements were conducted on a BesTec (Germany) X-ray photoelectron spectrometer with an Al Kα source. The samples were characterized with a field-emission scanning electron microscope TESCAN MIRAIII (Czech). Transmission electron microscopy (TEM) images were acquired with a field-emission JEOL 2100F operating at 200 kV. The specimens were prepared by cutting a slice of the QT-300 solid with Ga^+ ions inside the chamber and transferring it to the TEM holder. The formula of QT-300 was calculated by digesting a powder sample (5 mg) in NaOH (2.5 mL, 2 M), and the resulting clear solution was diluted to 100 mL and adjusted to a pH of 7 with HCl. A simultaneous inductively coupled plasma optical emission spectrometer (Varian Vista-PRO, Springvale, Australia) with a radial torch coupled to a concentric nebulizer and Scott spray chamber and equipped with a charge-coupled detector was used for ICP measurements. Leaching of cobalt from the QT-300 sample in water was analyzed by ICP at the end of the tandem reactions. Temperature-programed desorption of NH_3 (NH_3-TPD) was measured using the Micromeritics TPD-TPR 2900 system equipped with a thermal conductivity detector. First, the desired amount of the catalyst was pretreated at 150 °C in He stream of 20 mL min^{-1} for 1 h, then cooled down to 40 °C, and subsequently exposed to ammonia (4 vol % in He, 20 mL min^{-1}) for 1 h. Then, the ammonia that does not bind to the catalyst was removed by additional purging with 20 mL min^{-1} of He within 30 min. Eventually, the

https://doi.org/10.1021/acssuschemeng.1c02851
ACS Sustainable Chem. Eng. 2021, 9, 10611−10619

desorption was performed by raising the temperature from 40 to 750 °C at a heating rate of 10 °C min^{-1} in He stream (20 mL min^{-1}).

Synthesis of $[Co_6(oba)_5(OH)_2(H_2O)_2(DMF)_4]_n$·2DMF (TMU-10). The synthesis of TMU-10 was performed as reported in the literature.[29] In brief, in a typical preparation procedure, the powder sample of TMU-10 was obtained by mixing oba (2 mmol) and $Co(NO_3)_2·6H_2O$ (0.578 g, 2 mmol) in 40 mL DMF in a round-bottom flask at 145 °C for 72 h. The resulting powder was isolated by centrifugation, washed 3 times with DMF, and dried in air before characterization. Yield: 0.841 g (89% based on oba ligand). IR data (KBr pellet, ν/cm^{-1}): 658(m), 782(m), 873(m), 1012(w), 1098(m), 1160(m), 1237(vs), 1398(vs-br), 1504(m), 1558(s), 1603(vs), 1661(vs), 2928(w) and 3417(w-br) (Figure S1). Elemental analysis (%) calculated for $[Co_6(C_{14}O_5H_8)_5(OH)_2(H_2O)_2(C_3NOH_7)_4]·(C_3NOH_7)_2$: C: 49.3, H: 4.1, N: 3.9; Found: C: 49.6, H: 3.9, N: 3.6.

Q-MOFs were obtained starting from TMU-10 by thermal treatment in air at a heating rate of 5 °C min^{-1} between 100 and 700 °C for a period of 1 h. The samples were denoted by QT-*x*, where "T" and "*x*" stand for TMU-10 and the temperature of thermal treatment, respectively. Analysis of the gases evolved upon heating at 300 °C was made with a gas chromatography (GC)−mass spectrometry (MS) Agilent quadrupolar analyzer.

Catalytic Activity. The aerobic oxidative synthesis of imine by cross-coupling of alcohol and amine was performed under solvent-free conditions by consecutively mixing benzyl alcohol (0.5 mmol), aniline (0.5 mmol), and a certain amount of the corresponding catalyst into a 25 mL reaction vessel equipped with a magnetic stirrer under open air at room temperature. Subsequently, a desired amount of the mixture was collected with a syringe and analyzed by gas chromatography with a flame ionization detector (GC-FID, Echrom GC A90). The conversion and yields were also obtained by GC based on the ratio of alcohol to imine as follows[5]

$$\text{conversion (\%) based on substrate} = [1 - ((\text{concentration of substrate at a given time}) \times (\text{initial concentration of substrate})^{-1})] \times 100 \quad (1)$$

After the completion of the reaction as determined by TLC and GC, the catalyst was separated by filtration and washed several times with methanol and deionized water and dried at 100 °C overnight under vacuum in order to remove volatile organic impurities, and then, the sample was reused in the next cycles under the same reaction conditions. Finally, the desired *N*-benzylidenaniline product was characterized by ^1H and ^{13}C NMR analysis (Figure S2).

RESULTS AND DISCUSSION

Characterization. Cobalt-based TMU-10 MOF, $[Co_6(oba)_5(OH)_2(H_2O)_2(DMF)_4]_n$·2DMF was synthesized in the gram scale by mixing of $Co(NO_3)_2·6H_2O$ and H_2oba as indicated in the literature.[29] This MOF is based on hexanuclear SBU, $Co_6(CO_2)_{10}(\mu_3\text{-}OH)_2(O)_4$ (Figure 1), with pores running along the *b*- (6.2 × 6.1 Å) and *c*-axes (9.6 × 4.3 Å). The structure has 32.7% void space per unit cell (Figure 1). The SBU contains three crystallographically independent Co(II) ions. All cobalt(II) ions are bound to six oxygen atoms, four from oba ligands, one to the μ_3-O atom of the OH^- anion, and other to the oxygen atom of H_2O or DMF molecules (Figure 1).

Based on thermogravimetric analysis (TGA) measurements, thermal calcination should produce the partial TMU-10 deligandation, probably with the generation of pores and creation of unsaturated Co^{2+} ions. For this purpose, eight different temperatures (i.e., 100, 150, 200, 250, 300, 350, 400, and 700 °C) were selected for thermal treatment of TMU-10 under air for 1 h. The process should remove solvents and a fraction of ligands. At temperatures up to 150 °C, two DMF guest molecules and one bonded water molecule from each of

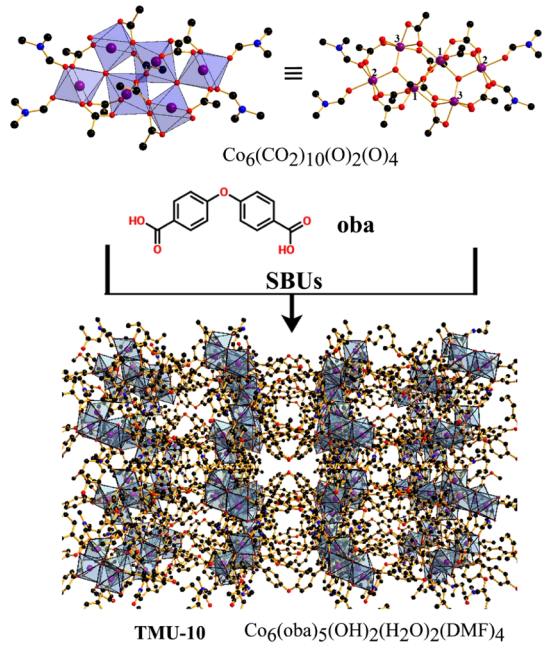

Figure 1. Single-crystal X-ray structure of TMU-10. Color code: O, red; N, blue; C, black; and Co, purple and blue polyhedra.

Co(3) centers are removed from the framework, making five coordinate Co(3) centers. Upon increasing the temperature at 200 °C, two DMF coordinated molecules to either of the two Co(2) centers were removed, forming four coordinated Co(2) centers. At 300 °C, two μ_3-O atoms of the framework OH^- anion are detached, resulting in Co(1), Co(2), and Co(3) with coordination numbers of five, three, and four, respectively (Figure S3). This proposal was supported by observation with GC−MS of evolution of H_2O and CO_2 in a 6 to 1 proportion when TMU-10 was heated at 300 °C after prior removal of DMF at 150 °C for 2 h.

The morphologies of TMU-10 and QT-300 samples were determined by FE-SEM. The images show that the TMU-10 sample is composed of nanoparticles (Figure S4a). Heating at 300 °C leads to agglomeration of the TMU-10 particles into larger particles observed for QT-300 (Figure S4b).

The evolution of the cobalt oxidation states and coordination from TMU-10 to QT-300 was determined by XPS (Figure 2). The XP spectrum of TMU-10 exhibits the peaks of Co $2p_{3/2}$ and Co $2p_{1/2}$ located at 780.5 and 796 eV with the corresponding intense satellite centered at 786.3 and 803 eV, respectively, all attributable to Co(II).[30] In the case of the QT-300 sample, four new peaks appeared at 779.6, 782.9, 789, and 804.5 eV were recorded. Since Co $2p_{3/2}$ has higher intensity and allows a better resolution of the individual components than the Co $2p_{1/2}$,[30] analysis of the distribution of Co sites was based on the deconvolution of the former peak. Curve-fitting of the Co $2p_{3/2}$ reveals that these new peaks can be ascribed to Co(III) $2p_{3/2}$ main peak, Co(II) in tetrahedral sites and two shake up satellites for Co(III), respectively, along with the decrease in the previous peak intensities of octahedral Co(II).[31,32] These results confirm that after deligandation, a portion of Co(II) centers is converted to Co(III), along with creating Co(II) in tetrahedral sites.

Variable-temperature PXRD of TMU-10 demonstrates that the crystal structure is retained up to 300 °C; the observed broadening of the diffraction peaks around 6−7° reflects the

https://doi.org/10.1021/acssuschemeng.1c02851
ACS Sustainable Chem. Eng. 2021, 9, 10611−10619

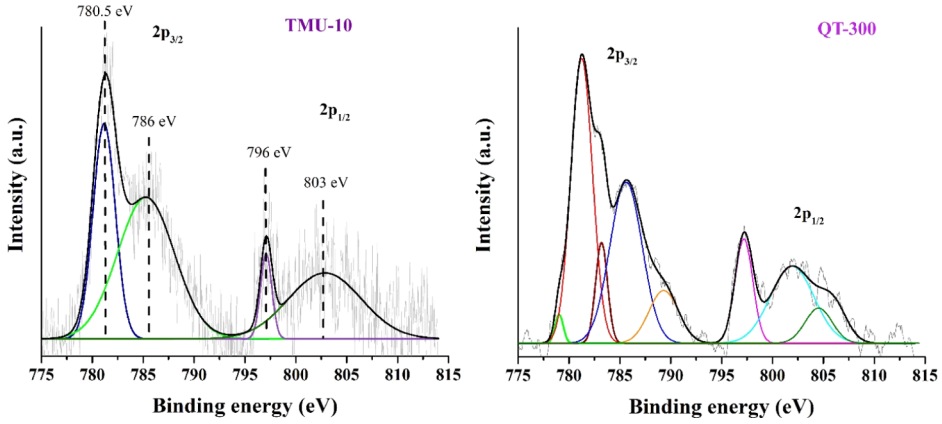

Figure 2. Fitted XP spectra of the Co 2p peaks for TMU-10 and QT-300 samples.

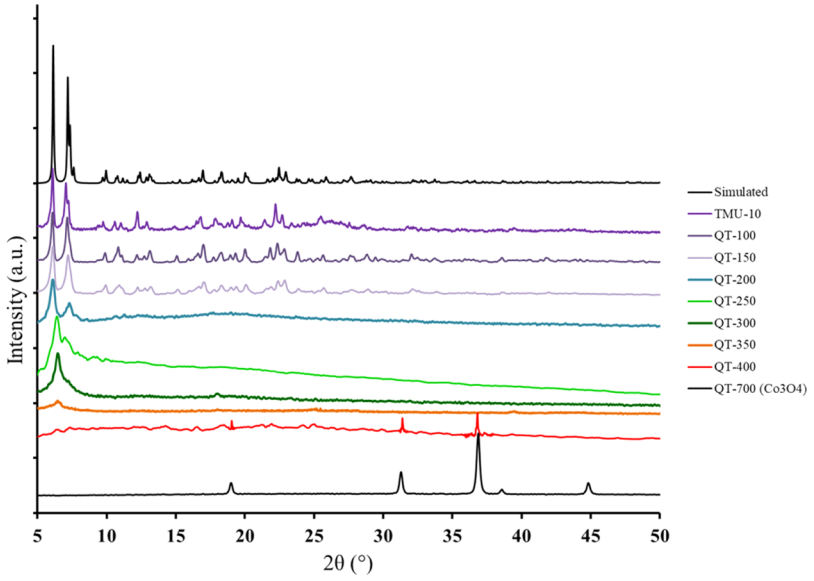

Figure 3. Comparison of PXRD patterns for simulated TMU-10, TMU-10, and QT-*x*.

partial deterioration of the TMU-10 crystal structure due to the creation of defects caused by deligandation (Figure 3). When the temperature rises to 350 °C, the characteristic peaks of TMU-10 significantly decrease in intensity, showing high degrees of structural collapse. The peaks corresponding to TMU-10 completely disappear upon treatment at 400 °C, while concomitantly, the diffraction peaks corresponding to Co_3O_4 related appear (JCPDS no. 42-1467), implying the complete decomposition of the TMU-10 framework at this temperature.

The evolution of porosity upon thermal treatment of TMU-10 was investigated by N_2 adsorption isotherms collected at 77 K for both TMU-10 and QT-300 (Figure 4). The data show that the BET surface area and total pore volume increase from 8.2 m^2/g and 0.023 cm^3/g for TMU-10 to 38.8 m^2/g and 0.157 cm^3/g in the case of QT-300, respectively (Table S1). The increase in the surface area and pore volume of QT-300 in comparison with TMU-10 can be attributed to the occurrence of partial deligandation and creation of vacant sites in the Q-MOF. Also, total mesoporous volume increases around 7.5 times from 0.019 cm^3/g for TMU-10 to 0.142 cm^3/g for QT-300, accompanied by a considerable growth in the adsorption at high relative pressures ($P/P_0 > 0.9$), indicating the presence of large cavities. Analysis of the BJH pore size distribution also corroborates the increase of pore width in QT-300 caused by thermal treatment (Figure 4). Therefore, thermal treatment of TMU-10 causes structural changes with generation of unsaturated metal sites in both micro- and mesopores, and these defects could be favorable from the catalytic point of view, enhancing the performance of QT-300 compared to TMU-10.

TEM images were taken by using Ga^+ to cut a slice of QT-300 thin enough to allow electron transmission. Figure 5 presents representative images of QT-300. These images revealed the nucleation of very fine CoOx nanoparticles on the outermost part of the crystallite and the observation of internal cavities within the QT-300 crystals. These two features are attributable to the effect of partial thermal degradation of the TMU-10 structure.

Catalytic Performance of QTMU-10 Samples for the One-Pot Alcohol Oxidation−Condensation. The one-pot synthesis of imines from alcohols and amines via tandem catalysis is an important and challenging process, involving oxidation and acid sites. Herein, the one-pot formation of *N*-benzylideneaniline from the cross-coupling of benzyl alcohol and aniline was chosen as the model reaction to evaluate the catalytic performance of QTMU-10. The reaction conditions

https://doi.org/10.1021/acssuschemeng.1c02851
ACS Sustainable Chem. Eng. 2021, 9, 10611−10619

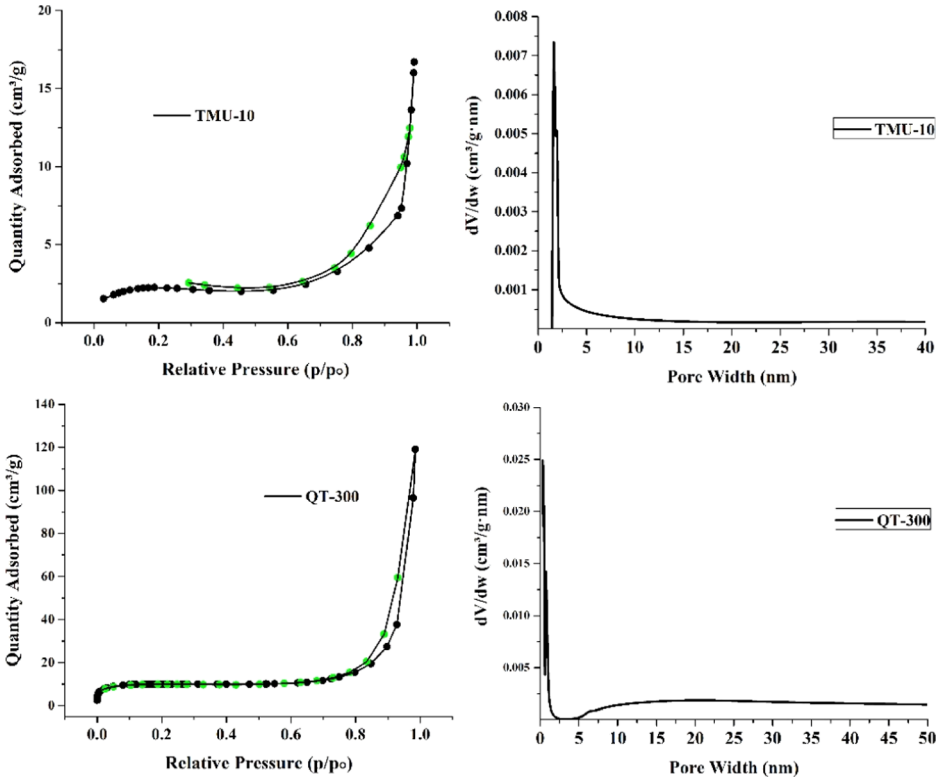

Figure 4. N_2 isotherm at 77 K and 1 bar and pore size distribution for TMU-10 and QT-300.

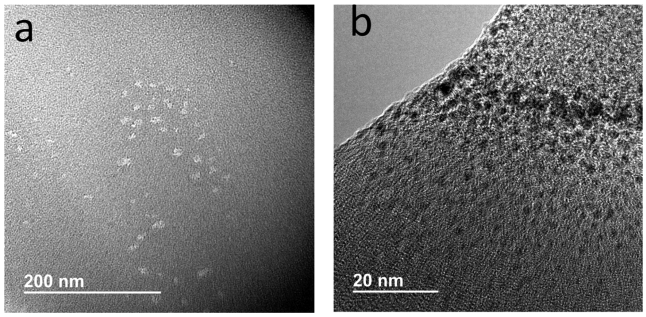

Figure 5. TEM images at two different magnifications taken upon cutting a thin slice of QT-300 with Ga^+-FIB, showing holes inside the lamella (a) and formation of very small CoOx nanoparticles in the outermost part of the QT-300 particle.

for the one-pot coupling of benzylic alcohol and aniline were optimized.

Effect of Deligandation Temperature. The effect of deligandation temperature on the catalytic efficiencies of various QTMU-10, that is, QT-100, QT-150, QT-200, QT-250, QT-300, QT-350, QT-400, and QT-700, for the one-pot synthesis of *N*-benzylideneaniline was investigated under solvent-free conditions under open air at 60 °C (Figure S5 and Table 1). When the reaction in the presence of QT-300 was performed at 60 °C in vacuum, the expected imine product was not observed and the alcohol oxidation did not happen without aerobic oxygen as the oxidant. However, under aerobic conditions and the presence of the QT-*x* catalyst, benzyl imine was formed at different reaction rates depending on the catalyst deligandation temperature. By increasing the deligandation temperature in the range of 250−300 °C, the reaction rate was enhanced and *N*-benzylideneaniline was formed at a shorter time. The optimal catalyst was QT-300

Table 1. Effect of Deligandation Temperature on *N*-Benzylidenaniline Yield Catalyzed by Various Q-TMU-10 MOFs[a]

catalyst	conversion time (h)	yield (%)
no catalyst	24	
QT-100	18	8
QT-150	18	32
QT-200	12	75
QT-250	4	92
QT-300	2	99
QT-350	10	28
QT-400	10	34
QT-700[b]	18	7

[a]Experimental conditions: catalyst mass = 2 mg, benzyl alcohol and aniline = 5 mL (0.5 mmol), T = 60 °C under open air. [b]Co_3O_4.

that renders higher yield and in half time than QT-250. Beyond the optimal deligandation temperature of 300 °C, the reaction rate and final imine yield decreased. This behavior can be explained considering the changes in both the pore structure and the content of coordinatively unsaturated active cobalt sites, as well as the formation of Co_3O_4. In the case of QT-200, with an intact pore structure and a limited density of open cobalt sites, a moderate increase in the catalytic activity was observed. Upon increasing the temperature up to 300 °C, the catalytic performance was enhanced notably and *N*-benzylideneaniline formation happened within a shorter time. The catalytic performance was drastically reduced from 350 to 700 °C, the tandem reaction taking place within a longer time. This trend can be explained based on the information provided by TGA, XRD, and XPS. At the deligandation temperature of 150 °C, the Co(3) center in the framework loses a coordinated H_2O molecule and a positive vacancy on the cobalt increases

https://doi.org/10.1021/acssuschemeng.1c02851
ACS Sustainable Chem. Eng. 2021, 9, 10611−10619

catalytic performance compared to the QT-100. In the case of the QT-200 sample, there are two unsaturated Co(3) centers (coordination number, CN = 5) and Co(2) due to the loss of two coordinated DMF molecules (CN = 4). In QT-250, the μ_3-OH ligand bridging the three cobalt centers, Co(1), Co(2), and Co(3), is partially removed, leading to enhanced catalytic performance in the tandem reaction. A more complete removal of μ_3-OH bridge ligand occurs after thermal treatment at 300 °C, and the QT-300 catalyst exhibits the best performance. This was confirmed by analysis of the gases evolved during the thermal treatment, whereby the presence of H_2O and CO_2 was observed. The enhanced catalytic activity is probably attributable to the synergistic effects of three unsaturated cobalt centers (1), (2), and (3) and simultaneous existence of meso- and micropores (in accordance with type I and IV curves) in the material. According to XRD, a major part of the QT-350 framework collapsed, resulting in a dramatic decline in catalytic activity. As the temperature increases further, the Co_3O_4 phase appears, being responsible for conversion in the QT-400 catalyst.

The density and strength of acid sites in parent TMU-10 and QT-300 were estimated using NH_3-TPD (Figure 6 and Table 2). Two NH_3 desorption peaks of TMU-10 appeared at 174 and 313 °C, which can be ascribed to acid sites of low and medium acid strength, respectively. In the case of QT-300, these peaks appeared at 174 and 331 °C. The TPD data indicate that the QT-300 catalyst has around threefold higher acid populations than its parent TMU-10. In other words, deligandation of TMU-10 at 300 °C leads to an increase in total acidity, most of which is related to the remarkable increase in medium-strength acid sites (see Figure 6). This acidity together with the higher surface area and porosity should be the reason why QT-300 exhibits the highest catalytic activity for the one-pot tandem imine formation.

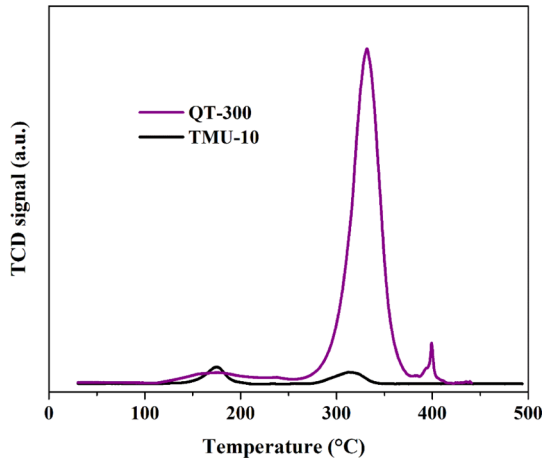

Figure 6. Temperature-programmed NH_3 desorption for TMU-10 and QT-300 catalysts.

According to the above results, QT-300 was chosen as the optimal QT-*x* catalyst for the tandem oxidation-coupling imine formation and was subsequently employed in additional catalytic studies.

Effect of QT-300 Catalyst Dosage. The influence of the amount of QT-300 on the rate of benzyl imine formation from benzyl alcohol and aniline was studied under open air as the green oxidant and under solvent-free conditions at 60 °C (Table 3). As shown in this table, there is no formation of benzyl imine in the absence of the catalyst. Upon addition of the QT-300 catalyst, the conversion percentage increased continuously. When 1 mg of QT-300 was introduced to the catalytic system, 75% conversion happened within 4 h, while higher conversion rates occurred over 2.5 mg of QT-300 in 1 h. However, by adding more QT-300 catalyst (>2.5 mg), the imine formation remained almost constant for the same time. Therefore, 2.5 mg was chosen as the suitable amount of the QT-300 catalyst in the subsequent experiments.

Table 3. Effect of QT-300 Mass on Benzyl Imine Synthesis[a]

entry	catalyst dosage (mg)	time (h)	conversion[b] (%)	yield[b] (%)
1	0	36		
2	1	4	75	74
3	1.5	3	87	86
4	2	2	98	98
5	2.5	1	99	99
6	3	1	99	99

[a]Experimental conditions: [benzyl alcohol] = 0.5 mmol and [aniline] = 0.52 mmol at 60 °C under open air. [b]Determined by GC.

In order to know the heterogeneous nature of the catalytic activity, QT-300 was separated from the reaction mixture at 40 min and the clear solution was transferred to a new vial, continuing the reaction in the absence of the catalyst for 4 h under the same reaction conditions. No additional conversion was observed in the absence of the catalyst after 40 min, indicating that the tandem reaction is promoted by QT-300 as a heterogeneous catalyst and that possible leached species do not contribute to the imine formation (Figure S6).

Effect of Alcohol on Amine Amounts. The influence of the amounts of benzyl alcohol and aniline on benzyl imine formation for a given mass of QT-300 was investigated (Table 4). As shown in Table 4, the highest imine formation was attained when the molar amounts of alcohol and aniline were 1:1.2. Beyond these amounts, the imine formation decreased significantly so that they reach the desired efficiency in a longer time (entries 6 and 7 compared to entry 5), probably due to the blocking of active surfaces of the catalyst with the reactants. Hence, the molar ratio of alcohol to amine was chosen as 1:1.2 in the next catalytic tests.

Effect of Temperature on Tandem Synthesis of Benzyl Imine. The effect of temperature on the formation of benzyl imine from benzyl alcohol and aniline catalyzed by QT-300 at various temperatures was evaluated (Figure S7 and

Table 2. Specific Density and Strength of Acidic Sites in TMU-10 and QT-300 Measured by NH_3-TPD Experiments

	weak acid		strong acid		
catalyst	peak position (°C)	value (mmol g^{-1})	peak position (°C)	value (mmol g^{-1})	total acidity (mmol g^{-1})
TMU-10	174	5.5	313	5.3	10.8
QT-300	174	0.6	331	31.8	32.4

https://doi.org/10.1021/acssuschemeng.1c02851
ACS Sustainable Chem. Eng. 2021, 9, 10611−10619

Table 4. Effect of the Alcohol and Amine Amount with Respect to QT-300 Mass for Optimal Imine Formation[a]

entry	benzyl alcohol (mmol)	aniline (mmol)	time (h)	alcohol to amine	conversion (%)
1	0.3	0.3	3	1:1	80
2	0.35	0.3	3	1.17:1	76
3	0.35	0.35	3.5	1:1	73
4	0.5	0.52	1	1:1.04	99
5	1	1.2	0.6	1:1.2	99
6	2	2.5	2	1:1.25	98
7	2	3	3	1:1.5	95

[a]Experimental conditions: *m* of the catalyst = 2.5 mg, *T* = 60 °C under open air.

Table 5). Upon increasing temperature from 25 to 80 °C, almost the same conversion was achieved in a much shorter time. Interestingly, the imine formation process takes place even at room temperature within 7 h in the presence of the QT-300 catalyst. Activity data indicate that QT-300 as a tandem aerobic oxidation-coupling catalyst is able to compete favorably with other reported catalysts (Table 6).

Table 5. Effect of Temperature on Imine Formation Catalyzed by QT-300

temperature (°C)	time (min)	conversion (%)
25	420	98
40	330	98
60	35	99
80	30	99

Possible Mechanism for Imine Formation over QT-300. Based on the literature data,[6,8] a likely mechanism for one-pot synthesis of *N*-benzylideneaniline from benzyl alcohol and aniline consists in the catalyzed aerobic oxidation of alcohol over QT-300 and subsequent Lewis acid-promoted condensation of the in situ-formed benzaldehyde in a one-step process.[6,8] The process occurring under open air and base-free conditions in the presence of the tandem catalyst of QT-300 is presented by eq 2.

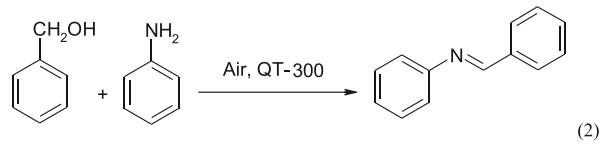

(2)

The rate-determining step in the tandem catalysis would be the aerobic oxidation. The process would take place in QT-300 due to the acceptable concentration of Co^{3+} centers and Co^{2+} in tetrahedral sites generated in the thermal treatment. The presence of both types of Co ions has been assessed by XPS. The proposed mechanism for the alcohol oxidation step is presented in Scheme 1.[6,37] Co^{3+} ions would act as redox sites, forming an alcoholate that would undergo oxidation, while Co^{3+} is reduced to Co^{2+}. Subsequently, the condensation step happens in the presence of aniline and benzaldehyde with the aid of the Lewis sites of QT-300. Thus, the key features of the mechanism are the intermediacy of benzaldehyde and the combined role of $Co^{III/II}$ redox centers and Lewis sites.

Scheme 1. Proposed Mechanism of Catalyzed Imine Formation over the QT-300 Tandem Catalyst

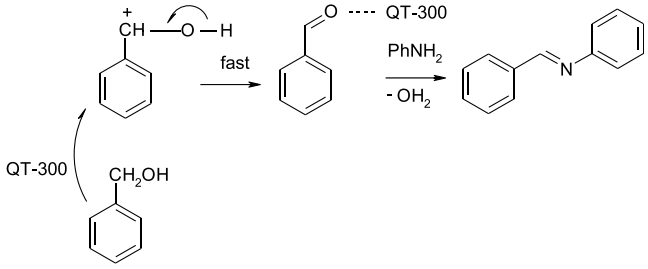

Reusability of the QT-300 Catalyst. In order to evaluate the reusability of the catalyst, the one-pot synthesis of benzyl imine was carried out for five consecutive runs using the same QT-300 sample, measuring the imine formation for each run. In addition, the conversion rate remained relatively unchanged after the fifth catalytic cycle, as observed in Figure S8a. Also, the framework of the QT-300 catalyst remained unaltered as seen in its XRD pattern (Figure S8b), indicating the stability of the tandem catalyst. These results indicate that the QT-300 is stable and can be reused in the tandem catalytic imine formation.

CONCLUSIONS

In this work, an efficient tandem catalytic process has been presented for *N*-benzylideneaniline synthesis by cross-coupling

Table 6. Comparison of the Catalytic Performance of QT-300 with Other Reported Catalysts for the Oxidative Cross-Coupling to *N*-Benzylideneaniline from Benzyl Alcohol and Aniline[a]

catalyst	solvent	oxidant	temperature (°C)	time (h)	conversion (%)	refs
9-azabicyclo [3.3.1] nonan-*N*-oxyl/KOH	toluene	air	80	4	92	33
$CoBr_2$	toluene	KO^{t}Bu	130	32	12	23
$MnCo_2O_4$-500	toluene	O_2	80	12	97.8	34
$MnCo_2O_4$-500	toluene	air	80	12	92.8	34
Co_3O_4	toluene	O_2	60	15		34
PICB-Au/Co	THF-TFE (9: 1)	O_2	30	12	53	35
MOF-1		air	100	12	89	26
Pd(OAc) 2/NEt 3/TEMPO		air	RT	72	75	36
CuI-TEMPO	CH_3CN	air	RT	12	74	3
Pd-Au@Mn(II)-MOF/KOH	toluene	air	110	30	99	25
quasi-TMU-10 (QT-300)		open air	60	0.6	99	this study
quasi-TMU-10 (QT-300)		open air	RT	7	98	this study

[a]TEMPO = 2,2,6,6-tetramethyl-1-piperidinyloxyl, TFE = 2,2,2-trifluoroethanol.

https://doi.org/10.1021/acssuschemeng.1c02851
ACS Sustainable Chem. Eng. 2021, 9, 10611−10619

of benzyl alcohol and aniline over quasi-cobalt-based MOF catalysts (QTMU-10) under green and mild conditions without the need of a solvent, base, and dehydrating agent. The QTMU-10 catalysts have been successfully synthesized by controlled thermolysis treatment under the air atmosphere at different temperatures ranging from 100 to 700 °C. The imine formation over QTMU-10 calcined at 300 °C exhibits the optimal catalytic performance, and its activity was investigated using various catalyst dosages, molar amounts of reactants, and reaction temperature. The synergistic effects of the uniform and extended distribution of coordinatively unsaturated cobalt positions across the framework and avoidance of particle agglomeration along with the simultaneous existence of micro- and mesopore structures (types I and IV) are proposed to be responsible for the improvement of the catalytic performance. The results show an economical and green approach for imine synthesis and highlight the great potential that controlled thermal treatment to create structural defects offer to develop MOF-derived catalysts with enhanced activity. Further extension and applications of cobalt-based quasi-MOF catalysts are in progress.

■ ASSOCIATED CONTENT

Supporting Information

The Supporting Information is available free of charge at https://pubs.acs.org/doi/10.1021/acssuschemeng.1c02851.

PXRD patterns, FESEM images, thermogravimetric profiles, and Fourier transform infrared spectra (PDF)

■ AUTHOR INFORMATION

Corresponding Authors

Mohammad Yaser Masoomi − *Department of Chemistry, Faculty of Science, Arak University, Arak 3848177584, Iran*; Email: m-masoomi@araku.ac.ir

Hermenegildo García − *Instituto de Tecnología Química, Universitat Politecnica de Valencia-Consejo Superior de Investigaciones Científicas, Universitat Politecnica de Valencia, Valencia 46022, Spain*; orcid.org/0000-0002-9664-493X; Email: hgarcia@upv.es

Authors

Minoo Bagheri − *Department of Chemistry, Faculty of Science, Arak University, Arak 3848177584, Iran*

Esther Domínguez − *Instituto de Tecnología Química, Universitat Politecnica de Valencia-Consejo Superior de Investigaciones Científicas, Universitat Politecnica de Valencia, Valencia 46022, Spain*

Complete contact information is available at: https://pubs.acs.org/10.1021/acssuschemeng.1c02851

Notes

The authors declare no competing financial interest.

■ ACKNOWLEDGMENTS

Support of this investigation by Arak University and Iran Science Elites Federation is gratefully acknowledged.

■ REFERENCES

(1) Sun, H.; Su, F.-Z.; Ni, J.; Cao, Y.; He, H.-Y.; Fan, K.-N. Gold Supported on Hydroxyapatite as a Versatile Multifunctional Catalyst for the Direct Tandem Synthesis of Imines and Oximes. *Angew. Chem., Int. Ed.* **2009**, *48*, 4390−4393.

(2) Cheng, S.; Ma, X.; Hu, Y.; Li, B. MnO_2/graphene oxide: A highly efficient catalyst for imine synthesis from alcohols and amines. *Appl. Organomet. Chem.* **2017**, *31*, No. e3659.

(3) Tian, H.; Yu, X.; Li, Q.; Wang, J.; Xu, Q. General, Green, and Scalable Synthesis of Imines from Alcohols and Amines by a Mild and Efficient Copper-Catalyzed Aerobic Oxidative Reaction in Open Air at Room Temperature. *Adv. Synth. Catal.* **2012**, *354*, 2671−2677.

(4) Tamura, M.; Tomishige, K. Redox properties of CeO_2 at low temperature: the direct synthesis of imines from alcohol and amine. *Angew. Chem.* **2015**, *127*, 878−881.

(5) Sithambaram, S.; Kumar, R.; Son, Y.; Suib, S. Tandem catalysis: Direct catalytic synthesis of imines from alcohols using manganese octahedral molecular sieves. *J. Catal.* **2008**, *253*, 269−277.

(6) Chen, B.; Wang, L.; Gao, S. Recent Advances in Aerobic Oxidation of Alcohols and Amines to Imines. *ACS Catal.* **2015**, *5*, 5851−5876.

(7) Zhang, Y.; Lu, F.; Zhang, H.-Y.; Zhao, J. Activated Carbon Supported Ruthenium Nanoparticles Catalyzed Synthesis of Imines from Aerobic Oxidation of Alcohols with Amines. *Catal. Lett.* **2017**, *147*, 20−28.

(8) Qiu, X.; Len, C.; Luque, R.; Li, Y. Solventless Oxidative Coupling of Amines to Imines by Using Transition-Metal-Free Metal−Organic Frameworks. *ChemSusChem* **2014**, *7*, 1684−1688.

(9) Corma, A.; García, H.; Llabrés i Xamena, F. X. Engineering Metal Organic Frameworks for Heterogeneous Catalysis. *Chem. Rev.* **2010**, *110*, 4606−4655.

(10) Masoomi, M. Y.; Morsali, A.; Dhakshinamoorthy, A.; Garcia, H. Mixed-Metal MOFs: Unique Opportunities in Metal−Organic Framework (MOF) Functionality and Design. *Angew. Chem., Int. Ed.* **2019**, *58*, 15188−15205.

(11) Dhakshinamoorthy, A.; Garcia, H. Catalysis by metal nanoparticles embedded on metal−organic frameworks. *Chem. Soc. Rev.* **2012**, *41*, 5262−5284.

(12) Bavykina, A.; Kolobov, N.; Khan, I. S.; Bau, J. A.; Ramirez, A.; Gascon, J. Metal−Organic Frameworks in Heterogeneous Catalysis: Recent Progress, New Trends, and Future Perspectives. *Chem. Rev.* **2020**, *120*, 8468−8535.

(13) Xu, C.; Fang, R.; Luque, R.; Chen, L.; Li, Y. Functional metal−organic frameworks for catalytic applications. *Coord. Chem. Rev.* **2019**, *388*, 268−292.

(14) Bagheri, M.; Masoomi, M. Y.; Morsali, A. High organic sulfur removal performance of a cobalt based metal-organic framework. *J. Hazard. Mater.* **2017**, *331*, 142−149.

(15) Kim, J.; Kim, S.-N.; Jang, H.-G.; Seo, G.; Ahn, W.-S. CO_2 cycloaddition of styrene oxide over MOF catalysts. *Appl. Catal., A* **2013**, *453*, 175−180.

(16) Dong, P.; Wang, H.; Liu, W.; Wang, S.; Wang, Y.; Zhang, J.; Lin, F.; Wang, Y.; Zhao, C.; Duan, X.; Wang, S.; Sun, H. Quasi-MOF derivative-based electrode for efficient electro-Fenton oxidation. *J. Hazard. Mater.* **2021**, *401*, 123423.

(17) Fan, L.; Zhao, F.; Huang, Z.; Chen, B.; Zhou, S.-F.; Zhan, G. Partial deligandation of M/Ce-BTC nanorods (M = Au, Cu, au-cu) with "Quasi-MOF" structures towards improving catalytic activity and stability. *Appl. Catal., A* **2019**, *572*, 34−43.

(18) Ryder, M. R.; Maul, J.; Civalleri, B.; Erba, A. Quasi-Harmonic Lattice Dynamics of a Prototypical Metal−Organic Framework. *Advanced Theory and Simulations* **2019**, *2*, 1900093.

(19) Wen, Y.; Zhang, J.; Xu, Q.; Wu, X.-T.; Zhu, Q.-L. Pore surface engineering of metal−organic frameworks for heterogeneous catalysis. *Coord. Chem. Rev.* **2018**, *376*, 248−276.

(20) Zhang, G.; Hanson, S. K. Cobalt-Catalyzed Acceptorless Alcohol Dehydrogenation: Synthesis of Imines from Alcohols and Amines. *Org. Lett.* **2013**, *15*, 650−653.

(21) Schwob, T.; Kempe, R. A Reusable Co Catalyst for the Selective Hydrogenation of Functionalized Nitroarenes and the Direct Synthesis of Imines and Benzimidazoles from Nitroarenes and Aldehydes. *Angew. Chem., Int. Ed.* **2016**, *55*, 15175−15179.

(22) Song, T.; Ren, P.; Duan, Y.; Wang, Z.; Chen, X.; Yang, Y. Cobalt nanocomposites on N-doped hierarchical porous carbon for

highly selective formation of anilines and imines from nitroarenes. *Green Chem.* **2018**, *20*, 4629−4637.
(23) Midya, S. P.; Pitchaimani, J.; Landge, V. G.; Madhu, V.; Balaraman, E. Direct access to N-alkylated amines and imines via acceptorless dehydrogenative coupling catalyzed by a cobalt(ii)-NNN pincer complex. *Catal. Sci. Tech.* **2018**, *8*, 3469−3473.
(24) Hazra, S.; Pilania, P.; Deb, M.; Kushawaha, A. K.; Elias, A. J. Aerobic Oxidation of Primary Amines to Imines in Water using a Cobalt Complex as Recyclable Catalyst under Mild Conditions. *Chem. Eur. J.* **2018**, *24*, 15766−15771.
(25) Chen, G.-J.; Ma, H.-C.; Xin, W.-L.; Li, X.-B.; Jin, F.-Z.; Wang, J.-S.; Liu, M.-Y.; Dong, Y.-B. Dual Heterogeneous Catalyst Pd−Au@ Mn(II)-MOF for One-Pot Tandem Synthesis of Imines from Alcohols and Amines. *Inorg. Chem.* **2017**, *56*, 654−660.
(26) Tan, J.-Y.; Shi, J.-X.; Cui, P.-H.; Zhang, Y.-Y.; Zhang, N.; Zhang, J.-Y.; Deng, W. A Ni3(OH)(COO)6—based MOF from C3 symmetric ligands: Structure and heterogeneous catalytic activities in one-pot synthesis of imine. *Micropor. Mesopor. Mat.* **2019**, *287*, 152−158.
(27) Pascanu, V.; González Miera, G.; Inge, A. K.; Martín-Matute, B. Metal−Organic Frameworks as Catalysts for Organic Synthesis: A Critical Perspective. *J. Am. Chem. Soc.* **2019**, *141*, 7223−7234.
(28) Dhakshinamoorthy, A.; Alvaro, M.; Garcia, H. Aerobic Oxidation of Benzyl Amines to Benzyl Imines Catalyzed by Metal−Organic Framework Solids. *Chemcatchem* **2010**, *2*, 1438−1443.
(29) Masoomi, M. Y.; Bagheri, M.; Morsali, A. Application of Two Cobalt-Based Metal−Organic Frameworks as Oxidative Desulfurization Catalysts. *Inorg. Chem.* **2015**, *54*, 11269−11275.
(30) Chuang, T. J.; Brundle, C. R.; Rice, D. W. Interpretation of the x-ray photoemission spectra of cobalt oxides and cobalt oxide surfaces. *Surf. Sci.* **1976**, *59*, 413−429.
(31) Fantauzzi, M.; Secci, F.; Sanna Angotzi, M.; Passiu, C.; Cannas, C.; Rossi, A. Nanostructured spinel cobalt ferrites: Fe and Co chemical state, cation distribution and size effects by X-ray photoelectron spectroscopy. *RSC Adv.* **2019**, *9*, 19171−19179.
(32) Biesinger, M. C.; Payne, B. P.; Grosvenor, A. P.; Lau, L. W. M.; Gerson, A. R.; Smart, R. S. C. Resolving surface chemical states in XPS analysis of first row transition metals, oxides and hydroxides: Cr, Mn, Fe, Co and Ni. *Appl. Surf. Sci.* **2011**, *257*, 2717−2730.
(33) Wan, Y.; Ma, J.-Q.; Hong, C.; Li, M.-C.; Jin, L.-Q.; Hu, X.-Q.; Hu, B.-X.; Mo, W.-M.; Sun, N.; Shen, Z.-L. Direct synthesis of imines by 9-azabicyclo-[3,3,1]nonan-N-oxyl/KOH-catalyzed aerobic oxidative coupling of alcohols and amines. *Chin. Chem. Lett.* **2018**, *29*, 1269−1272.
(34) Huang, X.; Liu, L.; Gao, H.; Dong, W.; Yang, M.; Wang, G. Hierarchically nanostructured MnCo2O4 as active catalysts for the synthesis of N-benzylideneaniline from benzyl alcohol and aniline. *Green Chem.* **2017**, *19*, 769−777.
(35) Soulé, J.-F.; Miyamura, H.; Kobayashi, S. Selective imine formation from alcohols and amines catalyzed by polymer incarcerated gold/palladium alloy nanoparticles with molecular oxygen as an oxidant. *Chem. Commun.* **2013**, *49*, 355−357.
(36) Jiang, L.; Jin, L.; Tian, H.; Yuan, X.; Yu, X.; Xu, Q. Direct and mild palladium-catalyzed aerobic oxidative synthesis of imines from alcohols and amines under ambient conditions. *Chem. Commun.* **2011**, *47*, 10833−10835.
(37) Chen, Z.; Liu, Y.; Liu, C.; Zhang, J.; Chen, Y.; Hu, W.; Deng, Y. Engineering the Metal/Oxide Interface of Pd Nanowire@CuOx Electrocatalysts for Efficient Alcohol Oxidation Reaction. *Small* **2020**, *16*, 1904964.

https://doi.org/10.1021/acssuschemeng.1c02851
ACS Sustainable Chem. Eng. 2021, 9, 10611−10619